

Motor-protein “roundabouts”: Microtubules moving on kinesin-coated tracks through engineered networks

John Clemmens,^a Henry Hess,^a Robert Doot,^a Carolyn M. Matzke,^b George D. Bachand^c and Viola Vogel^{*a}

^a Department of Bioengineering and Center for Nanotechnology, University of Washington, Box 351721, Seattle, WA 98195, USA. E-mail: vvogel@u.washington.edu; Fax: 206 685 4434; Tel: 206 543 1776

^b Microdevice Technologies, Sandia National Laboratories, PO Box 5800, MS 0603, Albuquerque, NM 87185, USA

^c Biomolecular Materials and Interfaces, Sandia National Laboratories, PO Box 5800, MS 1413, Albuquerque, NM 87185, USA

Received 6th January 2004, Accepted 11th February 2004

First published as an Advance Article on the web 27th February 2004

Nanotechnology promises to enhance the functionality and sensitivity of miniaturized analytical systems. For example, nanoscale transport systems, which are driven by molecular motors, permit the controlled movement of select cargo along predetermined paths. Such shuttle systems may enhance the detection efficiency of an analytical system or facilitate the controlled assembly of sophisticated nanostructures if transport can be coordinated through complex track networks. This study determines the feasibility of complex track networks using kinesin motor proteins to actively transport microtubule shuttles along micropatterned surfaces. In particular, we describe the performance of three basic structural motifs: (1) crossing junctions, (2) directional sorters, and (3) concentrators. We also designed track networks that successfully sort and collect microtubule shuttles, pointing the way towards lab-on-a-chip devices powered by active transport instead of pressure-driven or electroosmotic flow.

Introduction

Microfluidics has had a tremendous impact on miniaturizing, automating, and integrating analytical systems for biology and chemistry. Utilizing nanoscale phenomena in analytical systems may further drive miniaturization and enhance detection to molecular levels. This study aims to show how biologically inspired nanotechnology can be integrated into synthetic devices that may lead to the next-generation of lab-on-a-chip designs.

In cells motor proteins are essential to the transport of cellular cargo and building of cellular components. Biological active transport molecules, such as the motor protein kinesin, are used in cellular systems for transport of nanoscale material in fluid environments, both for assembly and positioning of cellular structures. Harnessing these proteins for movement and assembly of synthetic components in a “molecular shuttle” will be useful for building nano-engineered materials. Motor proteins can increase transport speeds of nanoscale cargo by orders of magnitude over diffusive transport[†], and this can be exploited to decrease analyte detection times or to drive non-equilibrium reactions. Biological active transport needs only a few molecules (and thus minimal chemical fuel) to drive movement. Consequently, cargo carried by motor proteins may be individually delivered and processed within a very small surface area. Other potential applications for motor-

protein-coated surfaces include programmed molecular-scale assembly and directed transport for self-healing material surfaces.

Controlling motor protein movement is the key to integrating active transport properties into devices. Thus far, the motion of motor proteins has been confined mainly along individual tracks.^{1–8} While we understand quantitatively how the shuttle system will perform on straight track segments,⁷ there is a lack of information about how to effectively connect track segments together through junctions. Therefore, our goal is to (1) design junctions of broad interest for engineering devices and (2) measure quantitatively how motor proteins move through each junction. Rigorous testing of track junctions will allow one to predict probabilistically how networks will transport microtubules, possibly in a coordinated manner. It will also uncover new junctions of practical use in devices (e.g. sorters, collectors).

For active transport on synthetic surfaces, microtubules glide along kinesin-coated tracks, powered by the hydrolysis of adenosine 5'-triphosphate (ATP) (Fig. 1A). Adaptation of traditional microlithographic techniques to engineer channels that selectively adsorb kinesin gives us the flexibility to design virtually any planar track shape. In these tracks, microtubules are guided along the tracks as they bend when pushed against the wall to remain in the bottom of the channel.⁶ Microtubules are fluorescently-labelled and can be monitored as they move along tracks through track junctions.

This paper describes three new types of junctions for controlling motion of filaments on motor protein-coated tracks that have significance for track networks in devices. Junctions were designed

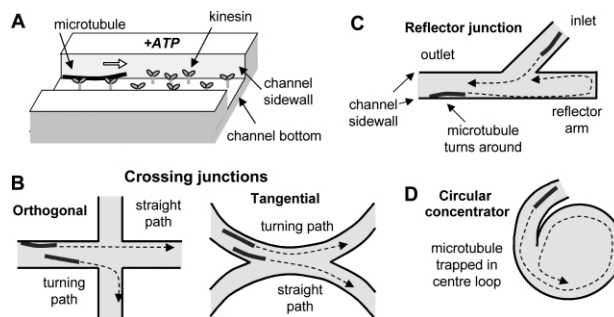


Fig. 1 Experimental detail of various track junctions. (A) The motor protein kinesin adsorbs at the bottom of microfabricated channels and translates microtubules. The track junctions investigated in this paper are (B) a crossing junction that allows microtubule tracks to cross one another at right angles (orthogonal crossing junction) or at shallow angles (tangential crossing junction), (C) the unidirectional reflector junction that traps and turns around microtubules in its arm, and (D) a circular concentrator that traps and collects microtubules in a centre loop. The channel bottom is coloured in grey with microtubule paths conceptually sketched by a dashed line.

[†] A 50 nm diameter particle requires 10-fold less time to move 100 μm by active transport than by diffusion. This assumes active transport moves at the speed of kinesin along microtubules ($\sim 1 \mu\text{m s}^{-1}$) and the particle has a diffusion coefficient in solution of $9.8 \times 10^{-12} \text{ m}^2 \text{ s}^{-1}$. Transport times for diffusion increase to the square of the distance, while active transport times only linearly increase with distance.

to give us control over the paths of microtubules as they glide through the intersecting tracks. These junctions are (1) crossing junctions (both orthogonal and tangential), (2) a unidirectional reflector, and (3) a circular concentrator as illustrated in Fig. 1. This study will foster a library of structural motifs that can serve as building blocks for engineering nanoscale assembly systems.

Experimental

Fabrication of tracks

Surfaces were prepared as previously described⁵ by patterning AZ5214 (Clariant, Somerville, NJ) on transparent 0211 glass substrate (Precision Glass & Optics, Santa Ana, CA). The photoresist was used for negative tone images of the chrome mask yielding 5 μm wide channels in a pinwheel pattern (Fig. 2A) and 2 μm and 5 μm wide channels in a spiral pattern as in Fig. 4. Channels with overhanging walls prevent microtubules from climbing the walls to escape the channel as discussed in our previous work.⁵ Surfaces were assembled into flow cells by sandwiching two Scotch double-coated tape spacers between an AZ5214 surface and a glass slide (Fishers Finest).

Microtubules and kinesin

Oregon-green (Molecular Probes, Eugene, OR) labelled microtubules (gift from J. Howard) and biotinylated microtubules (Cytoskeleton, Denver, CO) were used in separate assays. Both were polymerised in 4 mM MgCl_2 , 1 mM GTP, 5% DMSO, in BRB80,⁹ and diluted 100-fold into Assay Buffer (10 mM Tris acetate – pH 7.5, 50 mM potassium acetate, 4 mM MgSO_4 , 1 mM EGTA) with 10 μM taxol. Experiments used a truncated kinesin (pPK124 construct generously provided by J. Howard) consisting of the *N*-terminal 559 residues of the wild-type *D. melanogaster* kinesin heavy chain with C-terminal His-tag. Kinesin was expressed in *E. coli* and purified using a Ni-NTA column.¹⁰ The eluent contained functional motors at a concentration of ~ 0.1 mM and was stored as stock solution after adding sucrose (5% final concentration) at -80°C .

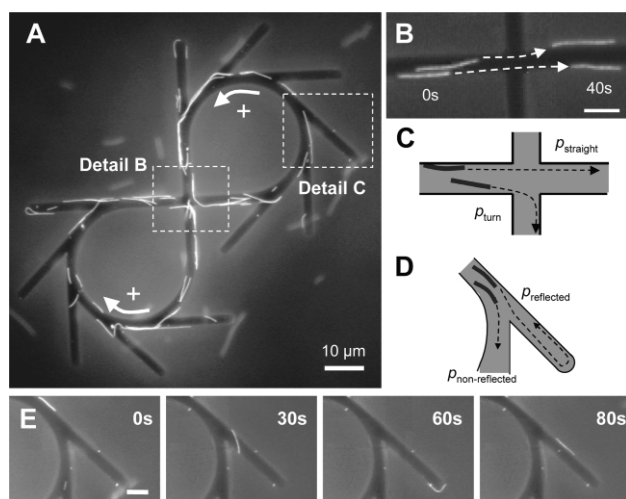


Fig. 2 (A) Sorting “figure 8”-shaped track comprised of (B) a crossing junction and (E) unidirectional reflectors. (B) Fluorescent microscope composite image showing two microtubules before (0 s) and after (40 s) crossing the junction. Dashed lines denote the paths of the microtubules. (C) In crossing junctions, microtubules generally continue straight through the intersection ($p_{\text{straight}} = 81 \pm 2\%$; fraction \pm standard error; $N = 89$ total events measured), while only a few microtubules are redirected along one of the perpendicular paths. (D) At unidirectional reflector junctions, microtubules were trapped in the arm more often than turning ($p_{\text{reflected}} = 67 \pm 7\%$ for each arm). (E) Sequential images showing a microtubule trapped in the reflector arm and bending around (60 s) to change its direction. Scale bar = 5 μm . In the “figure 8” pattern, approximately 93% of the microtubules in the loop travelled in the positive (+)-direction (observed after 30 min). Some microtubules were removed in (B) and (E) for clarity. (B), (E) Scale bars = 5 μm .

Motility assay

Protein solutions exchanged in flow cells followed those developed by Hiratsuka and coworkers⁴ with some modifications. Flow cells were filled with a kinesin solution [stock solution diluted tenfold in Assay Buffer with 0.05% Triton X100, 10 μM MgATP, and 0.02 mg ml^{-1} casein]. After 3 min, unbound kinesin was washed out by exchanging the solution for Assay Buffer with 0.05% Triton X100 and 10 μM MgATP. The remaining surface was pacified for 3 min using a blocking solution of Assay Buffer with 0.2 mg ml^{-1} casein and 10 μM MgATP. A microtubule solution (20 μM tubulin) in Assay Buffer with 10 μM taxol, 10 μM MgATP, and 0.02 mg ml^{-1} casein was added and incubated for 10 min. Finally, a Motility Solution [Assay Buffer with 0.02 mg ml^{-1} casein, 1 mM MgATP, 10 μM taxol, and an oxygen-scavenging system (20 mM DTT, 0.02 mg ml^{-1} glucose oxidase, 0.008 mg ml^{-1} catalase, 20 mM D-glucose; to prevent photobleaching)] was added.

Gliding motility of microtubules was imaged with an epifluorescence microscope (Leica DMIRBE) equipped with a 100 \times oil objective (N.A. 1.33) and a cooled CCD camera (Hamamatsu Orca II). Images were captured onto a Mac G3 workstation using Openlab software (Improvision, Coventry, UK).

Results and discussion

Crossing junction

Understanding transport along tracks that cross one another will become increasingly important as complex track networks are miniaturized. The simplest junction consists of two track segments crossing orthogonally or tangentially (Fig. 1B). The track segments tested were 5 μm wide channels. After addition of kinesin, microtubules, and finally the ATP-containing motility solution, microtubules were tracked as each crossed the intersection. For orthogonal crossings as in Fig. 2B, we found that most microtubules crossed straight through the intersection ($p_{\text{straight}} = 81 \pm 2\%$; fraction \pm standard error; $N = 89$ total events measured). Only rarely did they collide with the wall on the crossing track to follow the track to the right or left through bending ($p_{\text{turn}} = 19 \pm 2\%$). Similarly, for circular tracks intersecting tangentially as in Fig. 3B,

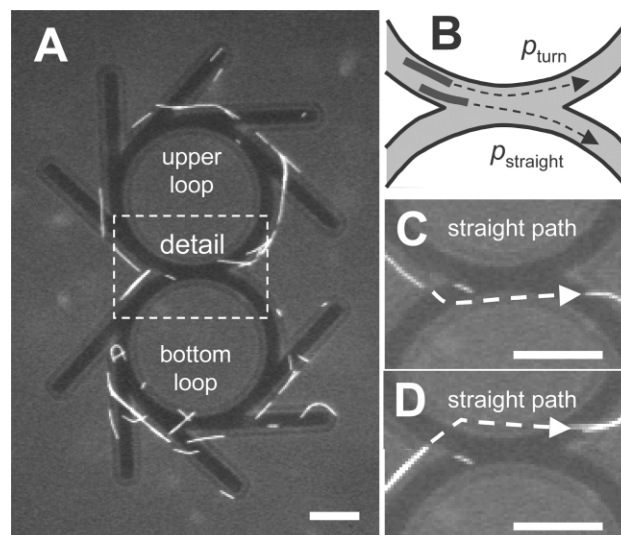


Fig. 3 (A) The “figure 8”-shaped track is comprised of two circular loops that form a tangential crossing junction and is decorated with unidirectional reflectors. (B) In a tangential crossing junction microtubules rarely turned to remain on the same circular loop ($p_{\text{turn}} = 21 \pm 5\%$; fraction \pm standard error; $N = 11$ events), but frequently travelled straight and switched to the other circular loop ($p_{\text{straight}} = 79 \pm 5\%$; fraction \pm standard error; $N = 41$ events). (C) Composite image showing microtubule position before and after passing through the tangential crossing junction. The microtubule shown follows a straight path (dashed line) to move from upper loop to bottom loop in the junction. (D) Similar composite image, illustrating microtubule moving from bottom to top loop. Some microtubules were removed from images (C) and (D) for clarity. Scale bars = 10 μm .

most microtubules travelled straight from one loop to the other ($p_{\text{straight}} = 79 \pm 5\%$; fraction \pm standard error; $N = 41$ events) rather than turning to stay on the same circular loop ($p_{\text{turn}} = 21 \pm 5\%$; fraction \pm standard error; $N = 11$ events). In junctions, microtubules were able to cross each other without changing their direction, suggesting that many motor protein-powered shuttles may be able to move simultaneously through crowded track networks and transport cargo with high throughput.

In the absence of any wall interactions, microtubule paths follow roughly straight paths over lengths of a few micrometres,⁷ thus favouring a straight path through both junctions. Based on measurements in our previous work⁷ a microtubule travelling a distance of $5 \mu\text{m}$ will deviate laterally $\sim 0.25 \mu\text{m}$ from its original direction on average. In the orthogonal crossing junction, approximately 5% of the microtubules will turn into the crossing track (Fig. 2C) assuming that microtubules deviate equally to the right and left, microtubules are aligned parallel to the channel, and microtubules are distributed evenly across the $5 \mu\text{m}$ channel width. This underestimates the actual probability of turning ($p_{\text{turn}} = 19 \pm 2\%$), most likely due to the fact that microtubules more often follow the walls and also are not necessarily aligned parallel to the channel centre. Similar arguments can be made for the tangential junction where a fraction of microtubules will deviate enough to turn and remain on the circular track. Unfortunately, though bound by material parameters of the microtubule structure (*i.e.* stiffness), individual microtubules turn stochastically. Therefore, detailed modeling will at best yield a probabilistic description of microtubule paths through junctions. Future efforts will attempt to model paths through arbitrary junctions and potentially suggest improvements to junction designs.

Directional sorting via reflector junctions

Directional control is crucial for motor proteins to be effectively utilized in devices. Direction of movement is determined by the microtubule polarity rather than the kinesin orientation on the surface. Along a single channel microtubules adsorbed from solution will move in both directions along the track. We were able to impart directionality to microtubules travelling into the junction by designing a short track segment, or “reflector”, shown in Fig. 1C. Microtubules travelling into the reflector were turned around when reaching the end of the segment, reversing its travel direction.

Reflector junctions were evaluated as single units with an inlet (upper segment in Fig. 1C), outlet (left segment in Fig. 1C), and a reflector arm segment and were arranged as in Fig. 2A. The offset angle of the inlet allowed microtubules to follow different paths depending on their approach direction. A microtubule approaching from the inlet would generally bend $\sim 45^\circ$ toward the outlet rather than turning $\sim 135^\circ$ into the reflector arm ($p_{45^\circ} = 97\%$ vs. $p_{135^\circ} = 3\%$; $N = 381$ events; 11 junctions). Microtubules entering from the outlet most often travelled into the reflector arm (Fig. 2E) rather than turning to the inlet ($p_{\text{reflected}} = 67\%$ vs. $p_{\text{non-reflected}} = 33\%$; $N = 39$ events), and microtubules entering from the reflector arm always travelled straight across the intersection to the outlet ($N = 35$ events).

While this design has been discussed conceptually as a Brownian ratchet,¹¹ the method of selectively adsorbing kinesin to only the bottom of channels vastly improved guiding efficiency and unidirectional movement over previously explored track schemes ($p_{\text{reflected}} = 67 \pm 7\%$; fraction reflected \pm standard error; $N = 26$ rectification events). These results are comparable to other reflector shapes⁴ and may be less sensitive to processing variations because simple straight track segments are used rather than arrowhead shapes. Further improvements on directional sorting may be possible by using thinner channels that better align the microtubule to the track axis⁷ thereby increasing the probability of trapping microtubules into the arms. This modified “T” junction may also

allow more freedom to “tune” the degree of sorting simply by changing the angle between inlet and outlet segments.

Reflector junctions were linked serially in a pinwheel pattern as shown in Fig. 2A. At steady state ($t > 30$ min), this pattern sorted the microtubules such that $\sim 93\%$ of the microtubules travelling along the “figure 8” looping track were moving in the same (+)-direction. Those moving in the opposite direction were due primarily to microtubules turning in the crossing junction. Unidirectional movement is important for devices containing areas that perform assembly tasks, where directionality along a track assures a specific assembly order.

Circular concentrator

In some cases cargo carried by molecular shuttles may need to be concentrated or collected at a central area on a surface for further modification or detection. While we initially designed a spiral pattern with increasing curvature to determine its effect on shuttle guiding, our experiments showed that we had created a circular trap for microtubules (Fig. 1D; Fig. 4C) in the spiral centre (Fig. 4E). Initially, microtubules bound to the kinesin-coated track travelled in equal numbers toward the spiral centre and the spiral exit. Microtubules moving toward the centre reached the circular trap and accumulated in the trap (Fig. 4E).

Trapping was made possible by an overhang of the channel sidewalls⁵ as observed in the spiral track cross-section (Fig. 4B). In the spiral centre, microtubules most often passed underneath the overhang and approached the next wall at an angle ($< 90^\circ$) that led to microtubule bending toward the spiral centre again (Fig. 4D; $p_{\text{recirculate}} > 90\%$ estimated from ~ 80 events), thus creating a circular trap. Occasionally a microtubule in the trap would bend to the right ($> 90^\circ$) to escape the trap and move toward the spiral exit

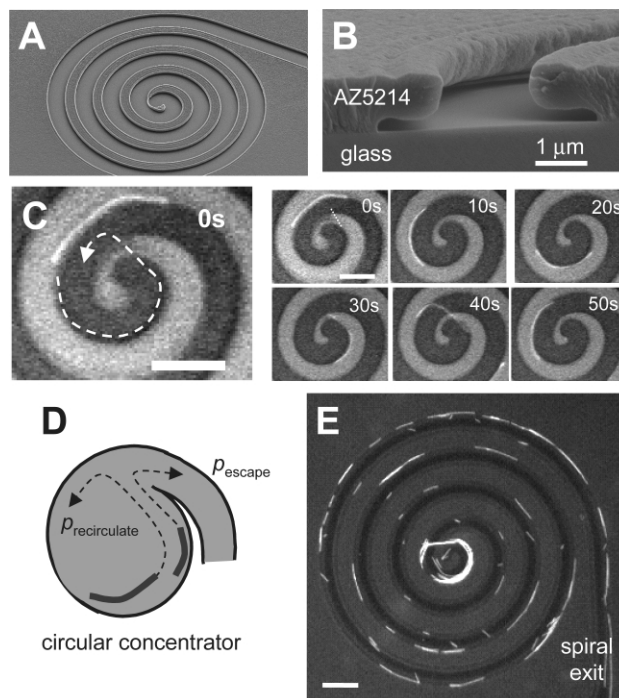


Fig. 4 Scanning electron micrographs show (A) the spiral pattern and (B) cross-section of the channel that include a $1 \mu\text{m}$ overhang of the channel sidewall. (C) Sequential fluorescent images showing fluorescent-labelled microtubule trapped in the circular concentrator junction. The tip of the spiral is a resist overhang (bright) connected to the glass surface (dark) at the dashed line. The overhang allows microtubules to pass underneath, collide with the wall at a shallow angle, and continue to circulate in the spiral centre. (D) Microtubules most often recirculated in the concentrator ($p_{\text{recirculate}} > 90\%$), while only rarely escaped ($p_{\text{escape}} < 10\%$). (E) After ~ 30 min microtubules continue to recirculate and accumulate in the circular concentrator at the spiral centre. The spiral exit is connected to a $\sim 8000 \mu\text{m}^2$ triangular area that feeds microtubules into the spiral pattern (not shown). Scale bars are $10 \mu\text{m}$ in (C) and (E).

($p_{\text{escape}} < 10\%$). Over time microtubules repeatedly recirculated in the trap and more microtubules accumulated as they entered the spiral centre (Fig. 4E). We also tested surfaces without the overhang and found that microtubules were not trapped in the centre but could bend 180° with $\sim 1\ \mu\text{m}$ curvature radius at the track end to change direction and retrace the spiral outward.

Collection of microtubules in this manner may have applications in biosensing where analytes are captured by microtubules and are carried to the centre of the spiral. Integrating these properties into sensor surfaces could potentially increase sensitivity and simultaneously reduce detection times. To extend this device's sensing and concentrating capabilities, the outermost loop of the spiral pattern was linked to a large open triangular area ($\sim 8000\ \mu\text{m}^2$) that bound microtubules and fed them into the spiral, thereby increasing the number of microtubules able to be trapped in the spiral centre. This approach demonstrates a possible scheme to increase capacity of collected analytes, and also shows how track junctions can control shuttle density.

Conclusion

We have characterized track junctions for motor protein-powered molecular shuttles. With this new detailed picture a better understanding of shuttle movement through track networks emerges. Physical properties that influence the deviation of a shuttle from a straight path play a key role in determining its efficiency in crossing an intersection. Because shuttles move along roughly straight paths through junctions, their density and directionality can be controlled using novel junction geometries.

Microfluidic devices may soon benefit from molecular active transport using reflector junctions to carry analytes in a single direction or circular concentrators to collect cargo for sensing or further modification. As we continue to improve our control over harnessing active transport, motor protein systems will become an effective tool in powering, building, and sensing in miniaturized devices.

Acknowledgements

The authors gratefully thank Emilie W. Clemmens for careful review of this manuscript and Greg Golden and Dong Qin from the Nanotech User Facility for help with electron micrograph images. J.C. was supported in part by a fellowship from the Center for Nanotechnology (UIF) and an IGERT fellowship from the National Science Foundation (NSF). H.H. was supported in part by the Alexander-von-Humboldt Foundation. This work was funded by NASA Grant NAG5-8784 and by DOE/BES grant DE-FG03-03ER46024. Sandia is a multi-program laboratory operated by Sandia Corporation, a Lockheed Martin Company, for the United States Department of Energy under contract DE-AC04-94AL85000.

References

- 1 D. V. Nicolau, H. Suzuki, S. Mashiko, T. Taguchi and S. Yoshikawa, *Biophys. J.*, 1999, **77**, 1126–1134.
- 2 J. A. Jaber, P. B. Chase and J. B. Schlenoff, *Nano Lett.*, 2003, **3**, 1505–1509.
- 3 S. G. Moorjani, L. Jia, T. N. Jackson and W. O. Hancock, *Nano Lett.*, 2003, **3**, 633–637.
- 4 Y. Hiratsuka, T. Tada, K. Oiwa, T. Kanayama and T. Q. Uyeda, *Biophys. J.*, 2001, **81**, 1555–1561.
- 5 H. Hess, C. M. Matzke, R. Doot, J. Clemmens, G. D. Bachand, B. C. Bunker and V. Vogel, *Nano Lett.*, 2003, **3**, 1651–1655.
- 6 J. Clemmens, H. Hess, R. Lipscomb, Y. Hanein, K. F. Bhringer, C. M. Matzke, G. D. Bachand, B. C. Bunker and V. Vogel, *Langmuir*, 2003, **19**, 10967–10974.
- 7 J. Clemmens, H. Hess, J. Howard and V. Vogel, *Langmuir*, 2003, **19**, 1738–1744.
- 8 R. Bunk, J. Klinth, L. Montelius, I. A. Nicholls, P. Omling, S. Tagerud and A. Mansson, *Biochem. Biophys. Res. Commun.*, 2003, **301**, 783–788.
- 9 J. Howard, A. J. Hunt and S. Baek, *Methods Cell Biol.*, 1993, **39**, 137–147.
- 10 D. L. Coy, M. Wagenbach and J. Howard, *J. Biol. Chem.*, 1999, **274**, 3667–3671.
- 11 H. Hess, J. Clemmens, C. M. Matzke, G. D. Bachund, B. C. Bunker and V. Vogel, *Appl. Phys. A*, 2002, **75**, 309–313.